

# Effective viscosity of polymer networks in the presence of cross-link slip

William McFadden

*University of Chicago, Biophysical Sciences Program, Chicago, IL 60615*

(Dated: 1 January 2014)

We are trying to describe the problem of what happens when cross-links relax stress in semi-flexible filament networks. We have addressed the problem using a simplified model in which cross-links are allowed to slip past one another in a drag-like manner. This model gives a prediction for the long timescale effective viscosity of the medium. We have verified our solution using computational models of filaments in the limit where persistence length is much longer than filament length. In this model, we find that network architectures and slip rates give rise to different modes of connectivity.

## I. INTRODUCTION

In previous work, crosslinks have been taken to be either perfectly rigid attachment points (HLM) or extended springlike structures (Taeyoon). In addition, any mechanism of detachment is either absent (HLM) or governed by full detachment and full reattachment events (Taeyoon, Broederz). In our model, we aim to create a more simple and general picture of crosslink stress relaxation based on an effective molecular friction between filament attachment points.

Reversible cross linking can give rise to drag-like coping between polymer filaments.(appendix and sources)

Connecting molecular models of friction and a simplification of force velocity relations for myosin motors on surfaces.

Previous researchers have introduced the concept of molecular friction to describe crosslink slip. We want to look at what such a model would produce in a larger network.

coarse-graining the microscopic details of . We explore a linear force-velocity relationship for crosslink slip.

Chemists have made synthetic systems that exhibit so called slide-ring cross-linking, but thus far this exact mechanism has not been seen in biological systems. However, (some garbage experiments from biophysical journal that I know must exist because people put bullshit in biophysical journal all the time) have shown that multivalent crosslinks can effectively slide under a load.

## II. THE MODEL

We use the minimal network (Mikado model) defined by a potential

$$\mathcal{H} = \frac{1}{2}\kappa \int ds (\nabla^2 \mathbf{u})^2 + \frac{1}{2}\mu \int ds \left( \frac{dl(s)}{ds} \right)^2 \quad (1)$$

Here,  $\mu$  represents an extensional modulus of a filament, and  $\kappa$  represents a bending modulus. We generate 2D networks of these semi flexible filaments by laying down filaments of length,  $L$ , with random position and orientation.

Although real cytoskeletal networks may exhibit non-negligible anisotropy, we choose to focus our attention on isotropic networks for simplicity. We define the density using the distance between crosslinks along a filament,  $l_c$ . A simple geometrical argument can be used to prove that the number of filaments needed to fill a domain of size  $2D \times D$  is  $4D^2/Ll_c$ , and that the length density is therefore  $1/l_c$ .

In the absence of crosslink slip, we expect the network to comprise a connected solid with a well defined elastic modulus given by HLM. These networks are only well-connected when the ratio of filament length to intercrosslink spacing,  $L/l_c$  is greater than 5.6. Near this percolation threshold, there are only locally connected domains, and discussions of global network properties becomes less reasonable. Additionally, as the filament density is increased beyond this point, there is another transition between non-affine bending and affine stretching of filaments, which changes the dominating term of the elastic modulus.

In departure from the previous models, we wish to incorporate relaxation of the networks stored stress by letting the attachment points slip. We do this by introducing a drag-like coupling between filaments.

$$\mathbf{F}_{\text{drag}} = \xi \cdot \int ds (\mathbf{v}(\mathbf{s}) - \mathbf{v}_0(\mathbf{s})) p(s) \quad (2)$$

This model therefore assumes a linear relation between applied force and the velocity difference between attached filaments. Obviously, non-linearities can arise in the presence of stretch dependent attachment kinetics as well as non-linear force extension of crosslinks. We address non-linear effects in the appendix. Assuming non-linear effects can be accounted for by changing the  $\delta\zeta$  term, the motion for the entire network is governed by a dynamical equation of the form

$$\int ds (\zeta \mathbf{v}_i(\mathbf{s}) + \xi \sum_j (\mathbf{v}_i(\mathbf{s}) - \mathbf{v}_j(\mathbf{s})) p_{ij}(s)) = \nabla \mathcal{H}_i \quad (3)$$

Although the general mechanical response of this system may be very complex, we wish to focus our attention on the linear order steady-state creep response of the system to an applied stress. To do this we introduce a fixed stress,  $\sigma$  along the midline of our domain.

$$F_{\text{total}} = \nabla \mathcal{H}_i + \sigma \cdot \delta(x - D) - \int ds (\zeta \mathbf{v}_i(\mathbf{s}) + \xi \sum_j (\mathbf{v}_i(\mathbf{s}) - \mathbf{v}_j(\mathbf{s})) p_{ij}(s)) \quad (4)$$

Here, the first term in the integral is the filament's intrinsic drag through its embedding fluid,  $\zeta$ , while the second comes from the drag-like coupling between filaments,  $\xi$ . Finally, we add a 0 velocity constraint at the far edges of our domain of interest. We assume that our network is in the "dry," low Reynold's number limit, where inertial effects are so small that we can equate our total force to 0. In addition, because we wish to probe the behavior of large scale network deformations, we are neglecting thermal fluctuations.

### III. ANALYTICAL RESULTS

We would like to calculate an estimate of the effective viscosity for a network described by our model. We carry this out by assuming we can apply a constant stress along a transect of the network. With moderate stresses, we assume the network reaches a steady state affine creep. In this situation, we would find that the stress in the network exactly balances the sum of the drag-like forces from crosslink slip. So for any transect of length  $D$ , we have a force balance equation.

$$\sigma = \frac{1}{D} \sum_{\text{filaments}} \sum_{\text{crosslinks}} \xi \cdot (\mathbf{v}_i - \mathbf{v}_0) \quad (5)$$

where  $\mathbf{v}_i(\mathbf{s}) - \mathbf{v}_j(\mathbf{s})$  is the difference between the velocity of a filament at it's crosslink point and the velocity of the filament to which it is attached. We can convert the sum over crosslinks to an integral over the length using the average density of crosslinks,  $1/l_c$  and invoking the assumption of (linear order) affine strain rate,  $\mathbf{v}_i - \mathbf{v}_0 = \dot{\gamma}x$ . This results in

$$\sigma = \frac{1}{D} \sum_{\text{filaments}} \xi \cdot \int_0^L ds (\mathbf{v}(\mathbf{s}) - \mathbf{v}_0(\mathbf{s})) \frac{1}{l_c} = \sum_{\text{filaments}} \frac{\xi \dot{\gamma} L}{l_c} \cos \theta \cdot (x_l + \frac{L}{2} \cos \theta) \quad (6)$$

Here we have introduced the variables  $x_l$ , and  $\theta$  to describe the leftmost endpoint and the angular orientation of a given filament respectively. Next, to perform the sum over all filaments we wish to convert this to an integral over all orientations and endpoints that intersect our line of stress. The max distance for the leftmost endpoint is the length of a filament,  $L$ , and the maximum angle as a function of endpoint is  $\arccos(x_l/L)$ . The linear density of endpoints is the constant  $D/l_c L$  so our integrals can be rewritten as this density over  $x_l$  and  $\theta$  between our maximum and minimum allowed bounds.

$$\sigma = \frac{1}{D} \int_0^L dx_l \int_{-\arccos(\frac{x_l}{L})}^{\arccos(\frac{x_l}{L})} \frac{d\theta}{\pi} \frac{\xi \dot{\gamma} L}{l_c} \cdot \frac{D}{L l_c} \cdot (x_l \cos \theta + \frac{L}{2} \cos^2 \theta) \quad (7)$$

Carrying out the integrals leaves us with a relation between stress and strain rate.

$$\sigma = \frac{4L^2 \xi}{\pi 3 l_c^2} \dot{\gamma} \quad (8)$$

We recognize that the term next to the strain rate is the effective viscosity  $\eta_{eff}$  at steady state creep. For extensional stresses, this constitutive relation for the rate of deformation allows us to write down an equation for the rate of network thinning.

$$\frac{\partial l_c}{\partial t} = l_c \dot{\gamma} = \frac{l_c \sigma}{\eta} \sim l_c^3 \frac{\sigma}{L^2 \xi} \quad (9)$$

We can see that the rate of network thinning accelerates as we would expect. When the network reaches some minimum connectivity we assume that it stops behaving as a continuum material.

$$\tau_{break} = \frac{\eta_{eff}}{2\sigma} \cdot \left(1 - \frac{l_c^2}{l_{break}^2}\right) \quad (10)$$

This provides us with an estimate of the timescale of catastrophic breakdown for a network with a given initial architecture and molecular drag.

We have neglected the induced alignment of filaments by the applied stress. Finally, we wish to extend this analysis to have some idea of the frequency dependence of the complex elastic modulus. I sure hope there is some way to do this.

#### IV. COMPUTATIONAL SIMULATIONS

Next, we wanted to test our analytical conclusions on a computational model. The technical details of the model can be found in the Appendix, but we summarize the main modeling points here.

For computational simplicity in these models, we assume that the bending rigidity,  $\kappa$ , is infinite, allowing us to model filaments as non-bending springs of rest length,  $L$ , and spring modulus  $\mu$ . In the appendix, we show that our result is not significantly different from the result for semi-flexible polymers.

We discretize the filaments such that the equations of motion becomes a coupled system of equations for the velocities of filament endpoints,  $\mathbf{x}$ . The drag-like force between overlapping filaments results in a coupling of the velocities of endpoints.

$$\mathbf{A} \cdot \dot{\mathbf{x}} = \mathbf{f}(\mathbf{x}) \quad (11)$$

where  $\mathbf{A}$  represents a coupling matrix between endpoints of filaments that overlap, and  $\mathbf{f}(\mathbf{x})$  is the spring force between two endpoints. We can then numerically integrate this system of equations to find the time evolution of the positions of all filament endpoints.

We generate a network by laying down filaments with random position and orientation within a domain of size  $2D$  by  $D$  with periodic boundaries. The external stress (shear or extensional/compressional) is applied to all filament endpoints falling within a fixed x-distance from the center of the domain. Finally, filament endpoints falling within a fixed x-distance from the edges of the domain are constrained to be nonmoving.

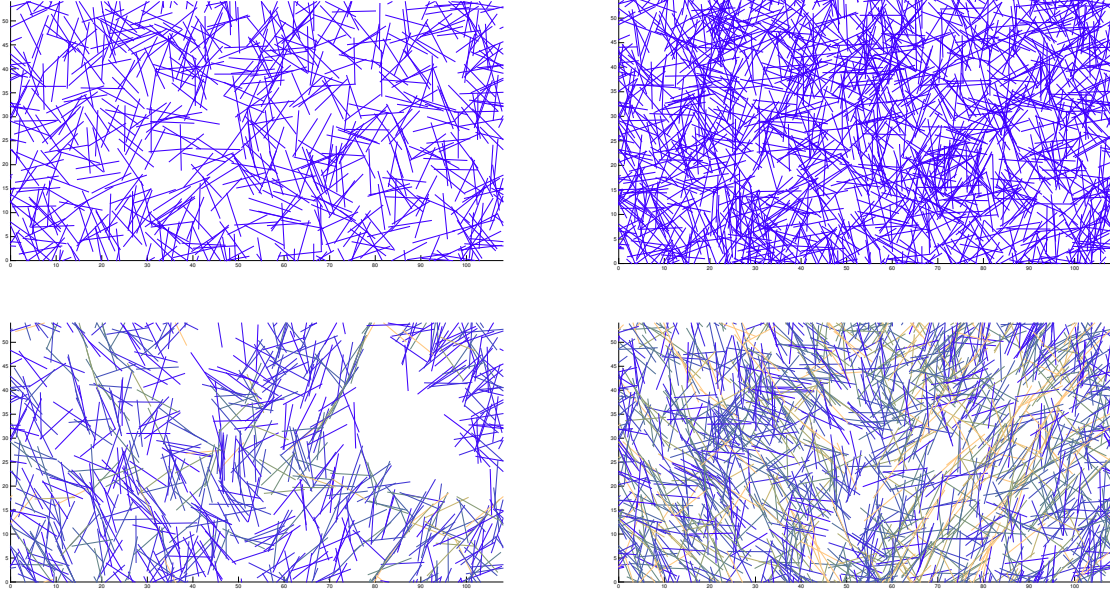


FIG. 1. Two Simulation setups with  $L = 9\mu m$ ,  $D = 54\mu m$  before and after 1000s of applied stress. a) low density  $l_c = 2\mu m$ , b) moderate density  $l_c = 1\mu m$

The nominal units for length, force, and time are  $\mu m$ , nN, and s, respectively. We explored parameters space around an estimate of biologically relevant parameter values, given in Table X.

All changes in the force felt by an endpoint are made smooth to allow integration of the differential equation (i.e. moving between stress domains, constraint domains, and overlap coupling occurs smoothly to prevent discontinuities). Parameter conditions that cause instabilities are excluded, and the endpoint trajectories are integrated out to at least 1000 seconds.

## V. SIMULATION RESULTS

Our computational simulations show that in the high density limit, our theoretical derivation is highly accurate at explaining the network behavior. However, we see that as the density of the network approaches the breakdown limit, the effective viscosity drops below our expected value.

This behavior depends strongly on the magnitude of total strain at the time of measurement and the crosslink coupling term.

This behavior is caused primarily by the low density network undergoing tearing events that interrupt global connectedness. It should be noted that in the low density limit, lower crosslink friction actually results in a smaller deviation from the theoretical prediction because it more easily allows re-annealing after tearing events. Meanwhile high crosslink friction causes steric avoidance after network segments are torn apart.

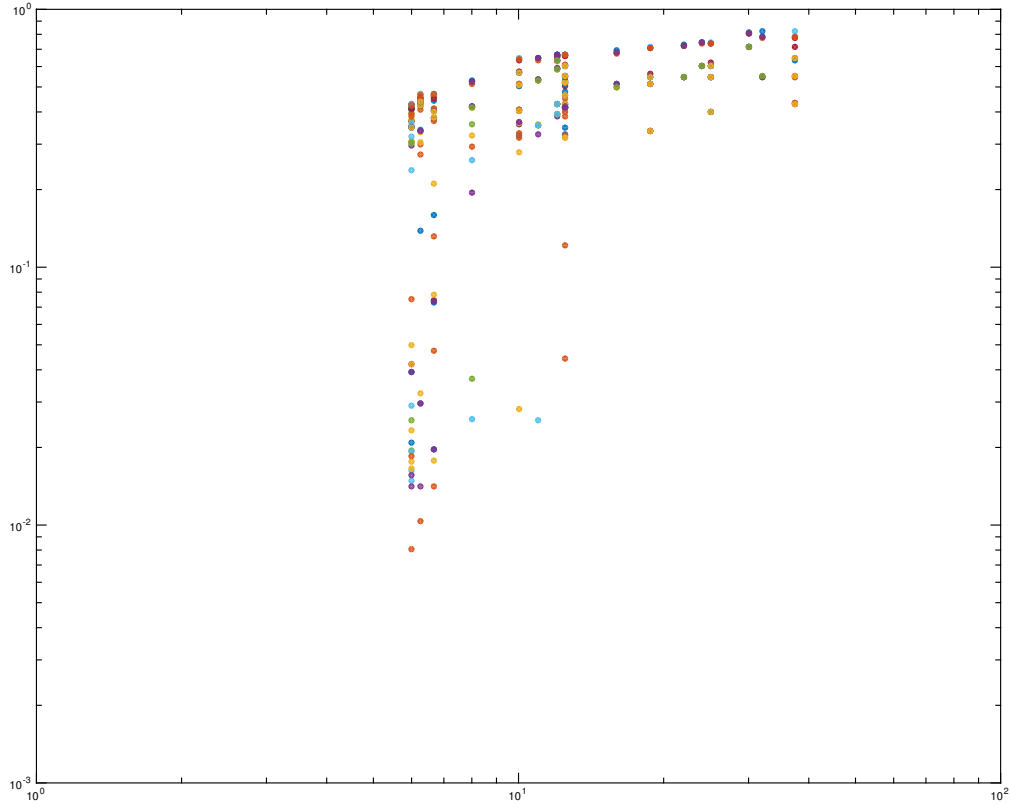


FIG. 2. Effective viscosity as a function of  $L/l_c$ .

For moderate strains, this result is largely the same as the result for extensional stress. However, at larger deformations, extensional networks tear apart at much lower

To further explore the occurrence of tearing events ...

Finally, we wished to explore the non-linear effects of reorientation of the filaments and non-linear network thinning/thickening. To do so, we applied oscillatory shear

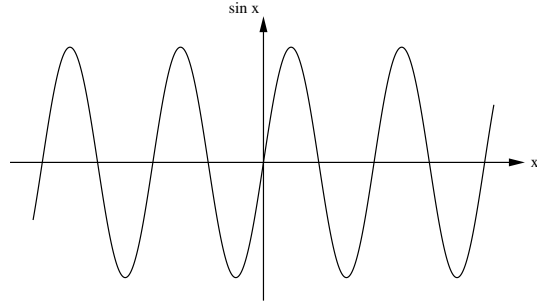


FIG. 3. Tearing rate as a function of  $L/l_c$ .

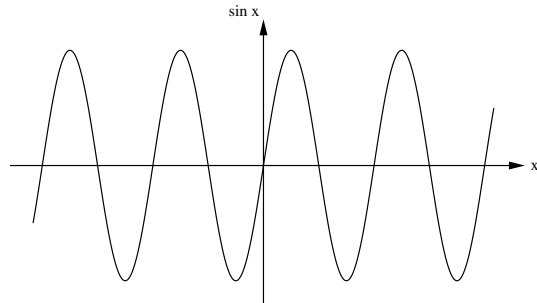


FIG. 4. Frequency dependence of elastic moduli.

## VI. DISCUSSION

Finally I wax philosophical, but who is going to pay for the ink?

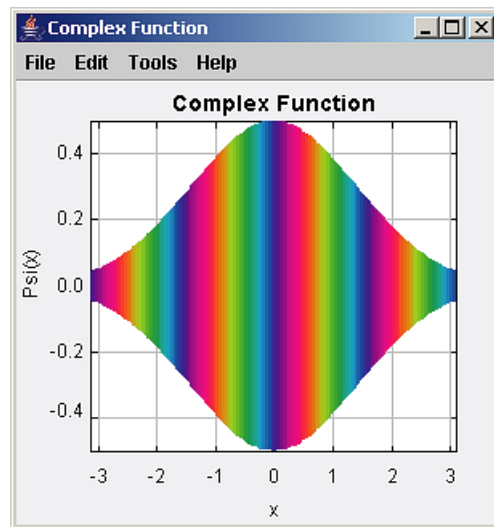


FIG. 5. Phase diagram of network connectivity.



## VII. APPENDIX A: DERIVING MOLECULAR DRAG COEFFICIENTS

Thus far, the idea of a molecular drag coefficient was taken as a phenomenological, measured parameter for a given experimental setup. While this is a sufficient pragmatic justification, it's useful to try to motivate the quantitative value of this drag coefficient by connecting it to the underlying cross-link properties of binding affinity, concentration, and extensibility.

To do this we'll imagine the simplified case of two cross linkers sliding past each other in one dimension. In this case, imagine that we have an equilibrium number of bound cross-linkers,  $n_B$ , each of which can be displaced from its equilibrium length by some distance  $x$ . Each cross linker unbinds with rate  $k_{off}$  and rebinds at it's relaxed position ( $x = 0$ ) with rate  $k_{on}$ . At the same time, all the cross linkers are being pulled from their relaxed position at a rate,  $v$ , which is simply the rate at which the filaments are sliding past each other.

We can right down an equation for the change in the density of cross-links as they are advected, bind, and unbind.

$$\frac{\partial \rho}{\partial t} = -k_{off}\rho(x) - v\frac{\partial \rho}{\partial x} + k_{on}\delta(x) \quad (12)$$

Recognizing that  $\int \rho(x) = n_B$  implies  $k_{on} = k_{off}n_B$ , we can find the steady state solution

$$\rho(x) = \frac{n_B k_{off}}{v} \cdot \exp\left(-\frac{k_{off}}{v}x\right) \quad (13)$$

If each cross-link has a spring constant  $\mu_c$ , then we can equate the force on all cross-links to the applied force that is sliding the filaments past each other. Realistically, the spring constant and binding affinity would be functions of the cross-link stretch, but here we are taking them as approximately constant.

$$\int_0^\infty \rho(x)\mu_c x dx = v \frac{\mu_c n_B}{k_{off}} = F_{app} \quad (14)$$

Therefore, the term next to  $v$ , (i.e.  $\frac{\mu_c n_B}{k_{off}}$ ) would be equal to our molecular drag coefficient,  $\xi$ . assuming, approximately 1-5 cross links per filament overlap, and using the following table of estimates pulled from Ferrer et al., we can chart the accuracy of this simple predictive model.

cross-linker type	dissociation constant ( $s^{-1}$ )	spring constant ( $nN/\mu m$ )	drag coefficient ( $\frac{nN \cdot s}{\mu m}$ )
$\alpha$ -actinin	0.4	455	200-1000
filamin-A	0.6	820	500-2500

### VIII. APPENDIX B: SIMULATION DETAILS

And I think I'll probably include all the gory details of how my simulations work since I'll be wanting to have direct references to the code.

```
double y0 = 10; // example of declaration and assignment statement
double v0 = 0;  // initial velocity
double t = 0;   // time
double dt = 0.01; // time step
double y = y0; // solved all problems
```